STUDY ON THE EFFECTS OF ELASTIC MODULUS OF CONSTRUCTIONS ON HEAT AND MASS TRANSFER OF GAS EXPLOSION

Shilin Lei [1,2], ***Yulong Duan*** [1,2*], ***Jun Long*** [1,2], ***Kaijun Xiang*** [3*], ***Liwen Liu*** [1,2], ***Zehuan Li*** [1,2], ***Ziyang Wen*** [1,2], ***Lulu Zheng*** [1,2]

(1. College of Safety Engineering, Chongqing University of Science and Technology, Chongqing, 401331, China.
2.Chongqing Key Laboratory for Oil and Gas Production Safety and Risk Control Technology, Chongqing, 401331, China.
3.Hainan Tuolite Technology Co., Ltd, Hainan 570100, China)

Abstract: *The factor of combustion and explosion remains one of the main constraints on coal mining and management. To clarify the impact of structural properties on the consequences of gas explosion disasters during coal mining, this article conducts a study on the impact of the elastic modulus of structures on gas explosion disasters. The research results indicate that in the case where structures with high elastic modulus must exist, the elastic modulus of the structure has minimal impact on the structure during the early stage of flame development. The area of flame front and the degree of deflagration also decrease with the increase of elastic modulus, but the disturbance degree of airflow and flame in the pipe increases with the increase of elastic modulus. The peak flame velocity at elastic modulus of 0.7 GPa and 2.8 GPa increased by 3.56% and 7.47% compared to elastic modulus of 0.18 GPa, respectively; The upstream overpressure peak increased by 24.63% and 42.52%; The downstream overpressure peak increased by 11.19% and 20.62%. The peak values of flame velocity and overpressure increase with the increase of elastic modulus, while the explosion intensity and pressure rise rate increase with the increase of elastic modulus. The explosion intensity index at elastic modulus 2.8 GPa is approximately 1.45 times that at elastic modulus 0.18 GPa. Therefore, it is necessary to choose structures with smaller elastic modulus as much as possible to achieve the best fire and explosion suppression effect.*

Keywords: *Coal mine roadway; Structures; Elastic modulus; Explosion disaster; Explosion proof facilities*

***Corresponding author.**
E-mail addresses: 2015014@cqust.edu.cn (Yulong Duan*).

39724374@qq.com（Kaijun Xiang **）

1 Introduction

Coal mines, as the world's main industrial energy source, are still one of the main factors restricting coal mining and management due to combustion and explosion [1]. To reduce the losses caused by explosion accidents during coal mining, domestic and foreign researchers have explored the characteristics of gas combustion and explosion, and developed barrier and explosion suppression technologies and facilities in coal mine tunnels [2-4] .

Due to the fact that methane is the main component of gas, a large number of scholars have studied the impact of a single rigid structure on methane combustion and explosion [5]. Duan Yulong [6] has studied that in the pipeline with a length of 100cm, the maximum attenuation amplitude of foam ceramics to the peak overpressure can reach 28.6%, and when the installation position of foam ceramics is 40 cm away from the ignition end, its suppression effect is better. The research results of Cui Jiaojiao show that when the double-layer metal foam has different pore structures (LP-SP model) from large to small, the suppression efficiency of explosion overpressure can reach more than 60%, which is 2-3 times of the pore structure (SP-LP model) from small to large [7]. Fengying Long [8] found that the thickness of foam copper was positively correlated with the oscillation frequency and amplitude of overpressure and the suppression effect of overpressure peak. Huang Chuyuan [9] concluded that the square shape of the structure has the most significant impact on flame propagation and explosion evolution.

As researchers gradually focus on the impact of the properties of explosion-proof structures on methane combustion and explosion flames and overpressure, flexible structures are also gradually being applied in explosion-proof scenarios. Yuan Bihe [10, 11] found that the maximum explosion overpressure and pressure rise rate of a 10cm long loofah can be reduced by 73.90% and 71.12% compared to the unfilled one. Yu Shuwei [12] obtained that although the flame velocity peak value under polyurethane sponge under the same BR increased with the increase of BR of the structure, the velocity peak value and overpressure peak value of lighter carbon plate still decreased, which inhibited the Helmholtz oscillation characteristics of pressure. At the same time, researchers have found that if the rigid and flexible structures mentioned above cannot achieve isolation and explosion suppression effects, it will lead to higher risk consequences, which brings new problems to the safety of coal mine tunnels [13].

In addition, explosion-proof structures with different elastic moduli often coexist in actual explosion scenarios, and there is currently very little research on the risk of combustion and explosion under the mixed conditions of the two types of explosion-proof structures. Therefore, conducting research on the impact of gas combustion and explosion disasters under structures with different elastic moduli is of great significance for the layout of explosion-proof facilities in the coal mining industry, and also provides theoretical reference for further improvement in the field of combustion and explosion prevention.

1 Experimental setup

1.1 Experimental Platform

The system consists by a methane gas cylinder, an explosion shock tube, a pressure sensor, a shock wave tester, a high-speed camera Phantom V710L, and related pressure and flame data acquisition software in Fig. 1. Among them, methane gas cylinder (purity 99%) and explosion shock tube (10 × 10 × 100 cm^3), shock wave tester (with 2 acquisition channels), high-speed camera, ignition switch and igniter, mass flow meter (with a range of 0-5L/min). The pressure collection system consists of pressure collection software Tytest Date Veiw and a testing host, set as a single collection, with a sampling time of 200 ms, a negative delay of 10 ms, and a sampling frequency of 50 k. As shown in Fig. 2, P1 and P2 are the upstream and downstream pressure detection points, respectively. The PCC flame acquisition software is from PCC 3.6 version, with a collection frequency of 2000 fps and a resolution of 1280 × 240 pixels, exposure time 490 μ s. The exposure index is 3200. The Strength of materials performance parameters of the three structures are shown in Table 1. To ensure the rigor of the experiment, all three materials were soaked with flame retardants and tested for flame retardancy. The selection of the elastic modulus of the structure is based on previous research, and the order of the elastic modulus is Polyurethane sponge < EPE Pearl foam < Carbon fiber board.

1.2 Testing process

Table 1 Materials characteristic

Materials	Polyurethane sponge	EPE Pearl foam	Carbon fiber board
Blocking Rate（BR）	0.4	0.4	0.4
Density（g/cm^3）	0.41	0.95	1.43
Thickness（cm）	1	1	1
Elastic modulu（GPa）	0.18	0.7	2.8

Table 2 Experimental Conditions

Conditions	Environment temperature (℃)	CH4 (%)	Structure arrangement（40cm：50cm）
（a）			Carbon fiber board：Polyurethane sponge
（b）	12	9.5	Carbon fiber board：EPE pearl foam
（c）			Carbon fiber board：Carbon fiber board

$$CH_4 + \frac{1+\phi}{\phi} \times (O_2 + 3.76N_2) \rightarrow CO_2 + 2H_2O + 7.52N_2 + \frac{1-\phi}{\phi} \times (O_2 + 3.76N_2) \quad (1)$$

$$\phi = \frac{m_{fuel}/m_{air}}{(m_{fuel}/m_{air})_{stoic}} = 9.52 \times \frac{V_{CH_4}}{V_{air}} \quad (2)$$

A large number of studies have shown that the peak of overpressure during combustion and explosion first increases and then decreases with the increase of methane concentration, and reaches its maximum at 9.5% methane concentration. As the BR of the structure increases, it

increases first and then decreases, and reaches the maximum value when the BR is 0.4 [8]. The distance between polyurethane sponge and light carbon plate was investigated, and it was found that the turbulence degree was the highest when the distance between structures was 10 cm. Therefore, the distance between obstacles was 10 cm, the BR of structures was 0.4, and the methane concentration was 9.5%. The volume fraction of methane was calculated by Formula (1) and Formula (2).

Polyurethane sponge EPE Pearl foam Carbon fiber board

Fig. 1 Structure Materials

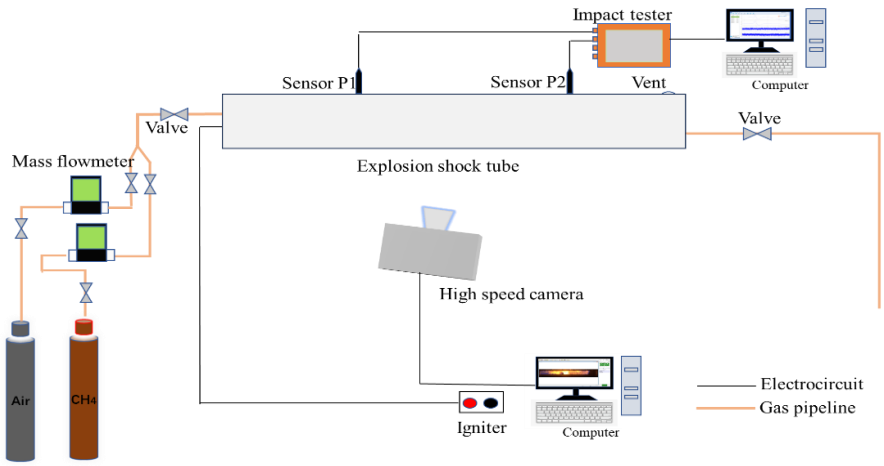

Fig.2 Experimental Platform

According to the pre-experimental results and relevant data representation, connect each device as shown in Fig. 2 and conduct the experiment according to Table 2. Inject air through the air compressor and check the airtightness of the device. Install each group in the designated position according to the experimental condition table. Repeat the inspection of the experimental device and fill it with methane air premixed gas with a volume fraction of 9.5% methane. After 8 minutes of ventilation using the 4-fold volume method, and let it stand for 1 minute, ignition is carried out and pressure and flame data are collected. Re-inlet the air and open the tail ball valve to exhaust the exhaust gas. Repeat each experiment at least 3 times to ensure the accuracy of the experiment.

2. Analysis of experimental results

2.1 Effect of Elastic Modulus of Structures on Methane Explosion Flame

Fig. 3 selects flames at the same time to clearly reveal the changes in the structure of gas explosion flames under three combinations of elastic modulus structures. The three combinations of structures have minimal impact on the early development stage of gas explosion flames, and the flames have all undergone spherical and finger shaped stages. The time required for the flame to develop to the first structure in conditions (a), (b), and (c) is 44.5 ms, 46 ms, and 46 ms, respectively. The time for the flame to develop to the second structure was 47.5 ms, 49 ms, and 49 ms, respectively. The delay in flame propagation time is attributed to the more frequent disturbance of structures with lower elastic modulus during the combustion and explosion process. In addition, an increase in elastic modulus can induce pressure and shock waves to tilt the entire structure. When the elastic modulus of the structure increases to a certain scale, the impact of flame and pressure does not cause deformation and tilting of the structure. The coupling effect of the structure causes flame instability, with wrinkles and vortices appearing at the flame front. At the same time, the flame front area and propagation efficiency decrease with the increase of elastic modulus (50.5 ms □ 53 ms).

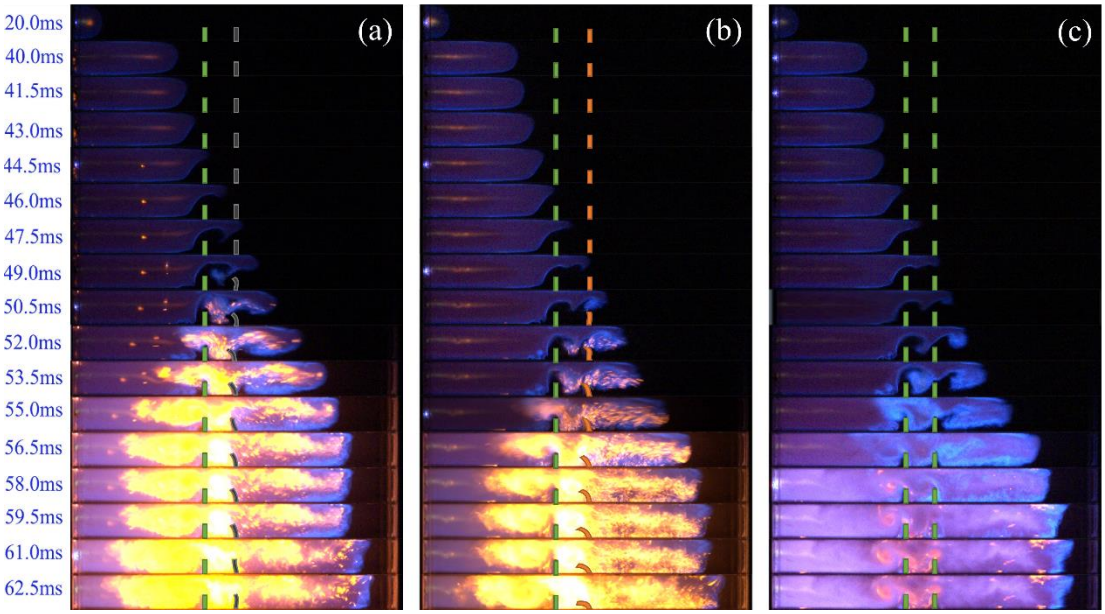

Fig. 3 the influence of the elastic modulus of the structure on the flame evolution process

The disturbance of the structure itself and its disturbance to the gas intensify the turbulence of the airflow in the burned area, while the rapidly turbulent gas forms a deflagration phenomenon due to the influence of high-pressure and high-temperature ignition sources [14]. This is because the disturbance of the structure enhances the thermal diffusion and convection efficiency caused by combustion from the burned zone to the unburned zone, providing support conditions for the occurrence of deflagration. The strength of the deflagration phenomenon is closely related to the elastic modulus of the structure, which also leads to the lowest degree of deflagration under condition (c), but severe turbulence is clearly visible, with the greatest risk and uncertainty of deflagration disasters [15, 16] . This also indicates that in situations where structures must exist,

such arrangements should be avoided as much as possible to reduce the consequences of gas explosion disasters.

2.2 Effect of elastic modulus on flame velocity

Select a time step of 5 ms and calculate the flame velocity according to formula (1) as shown in Fig. 4. T_2 is the termination time when the flame tip appears, T_1 is the initial time when the flame tip appears.

$$V = \frac{\Delta L}{T_2 - T_1} \tag{3}$$

The times of flame velocity peak in Fig. 4 are 50 ms, 55 ms, and 55 ms, respectively, which is consistent with the time taken for the flame to reach the first and second structures. The flame velocity image better reflects the change process of flame velocity, and the acceleration mechanism of structures with different elastic moduli before reaching the peak flame velocity is also inconsistent. Observing the gray box, it can be seen that the slope of the two point line connecting flame velocity in working condition (a) to working condition (b) and then to working condition (c) increases, and the induced velocity peak is the smallest in working condition (a), The maximum flame velocities of condition (b) and condition (c) increased by 3.56% and 7.47% respectively compared to condition (a), indicating that the acceleration mechanism of flame propagation becomes stronger with the increase of elastic modulus. This is because the flexible structures in working conditions (a) and (b), under the action of combustion and explosion flames and high pressure, the curl of the structure and its own fine porous structure attenuate some shock waves and energy [17].

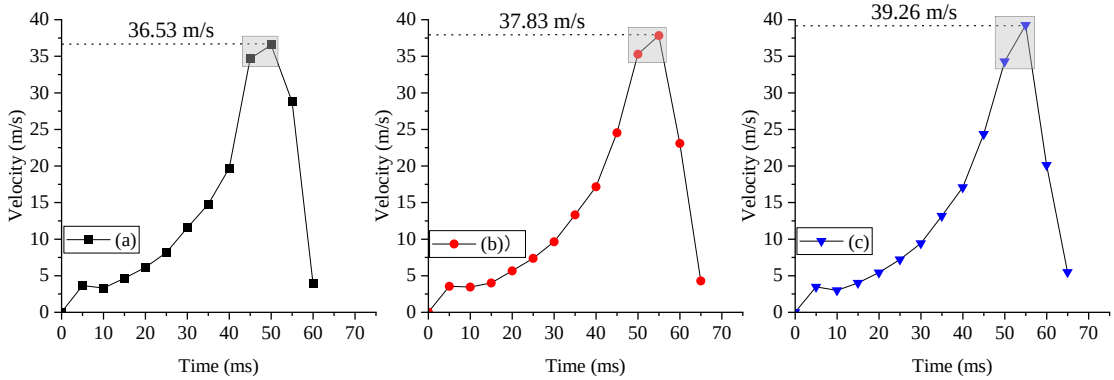

Fig. 4 Flame front propagation speed

2.3 Analysis of explosion overpressure effects on structures with different elastic modulus

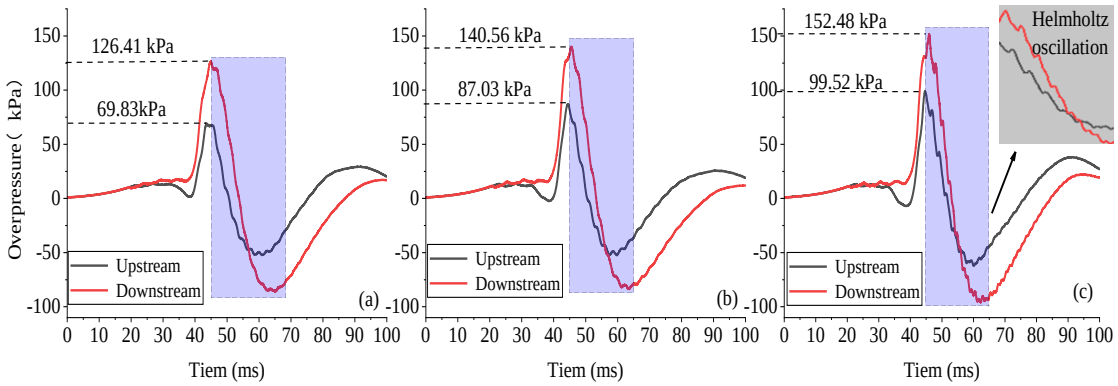

Fig. 5 Pressure time history curve under various operating conditions

The elastic modulus of a structure represents its ability to resist damage such as tension and bending, and the degree of damage to the structure can be expressed in terms of explosion strength. The value of explosion strength (explosion strength index) is equal to the product of the peak explosion overpressure and its pressure rise rate. Fig. 5 shows the pressure time history curves under three working conditions. The pressure rise rate and explosion intensity index calculated based on the peak overpressure are shown in Fig. 6. Based on Fig. 5 and Fig. 6, it can be seen that the evolution trend of the pressure curve is generally similar, with the maximum explosion pressure still appearing downstream. However, the pressure in the upstream region of condition (b) and condition (c) increased by 24.63% and 42.52% respectively compared to condition (a). For the downstream region, the pressure increased by 11.19% and 20.62% respectively, indicating that with the increase of elastic modulus, the peak pressure collected for both upstream and downstream increased.

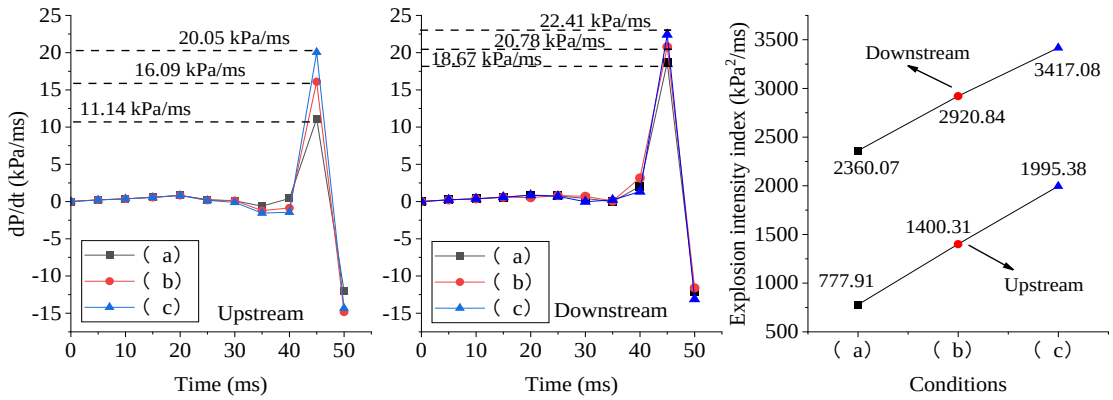

Fig. 6 Pressure rise rate and explosion intensity variation gauge

Secondly, due to the disturbance of the structure itself and the disturbance of the airflow and flames, the combustion efficiency is increased to a certain extent [17]. The heat generated by combustion diffuses and propagates in multiple directions and positions, coupled with the interaction between sound and pressure, the shock wave undergoes multiple reciprocating impacts,

resulting in an oscillating attenuation trend of the decrease in pressure after reaching the peak overpressure, known as the Helmholtz oscillation characteristic, which can be clearly seen, The pressure time history curve of working condition (a) is smoother than that of working condition (c), and this oscillation phenomenon becomes more significant as the elastic modulus increases [18, 19]. In the presence of a structure, when the elastic modulus is small, the structure can not only achieve a coupling mechanism for pressure attenuation, but also avoid multiple reciprocating impact injuries caused by pressure shock waves.

In the comparison of upstream and downstream pressure rise rates under the same working condition, it can be concluded that the rate of rise of downstream detonation pressure is higher than that of upstream. In the same pressure collection area, as the elastic modulus of the structure increases, the rate of pressure rise also gradually increases. The comparison of the explosion intensity index is also consistent with the pressure rise rate, both of which indicate that the explosion intensity generated downstream is the highest and the degree of damage caused is also the greatest. The explosion intensity index of working condition (c) is the maximum, and the explosion intensity index of working condition (a) is the minimum. The explosion intensity value of working condition (c) is about 1.45 times that of working condition (a). Further indicates that in the construction work of gas explosion prevention and control facilities, it is necessary to avoid the coexistence of structures with higher elastic modulus as much as possible, and structures with lower elastic modulus should be selected to form explosion prevention and control facilities.

3.Revealing the Influence Mechanism of Elastic Modulus Structures

The impact of shock waves and flames causes different degrees of tilting and local deformation of structures with different elastic moduli. Fig. 7 clearly reveals the process of the structure being subjected to the action of flames and shock waves. In Fig. 7 (a), due to the small elastic modulus of the structure, the local and overall resistance to deformation is extremely weak. The impact of shock waves on the structure results in local left and local right irregular distortion of the entire structure [12]; Secondly, there are varying degrees of unevenness on the left and right surfaces of the structure; The structure is impacted by flames, and some small flames enter the pores inside the structure to undergo quenching effect [5], absorbing some of the heat brought by the flames [20], resulting in the lowest flame velocity and overpressure peak formed under this elastic modulus of the structure. In Fig. 7 (b), the local irregular distortion phenomenon and the degree of unevenness on the surface of the structure will gradually decrease, and the ability of the structure to resist shock waves will be strengthened due to the increase in elastic modulus. However, due to the high density of the structure, the small pores weaken the ability of the flame to penetrate the surface of the structure, and quenching will occur in a very short time after penetration [21]. The elastic modulus of the structure in is already fully resistant to local and overall deformation, and small flames will completely lose the possibility of penetrating the surface of the structure from Fig. 7 (c). Due to the continuous disturbance of heat and shock waves generated by combustion and explosion accumulation, the flame velocity and overpressure peak under operating conditions are the maximum.

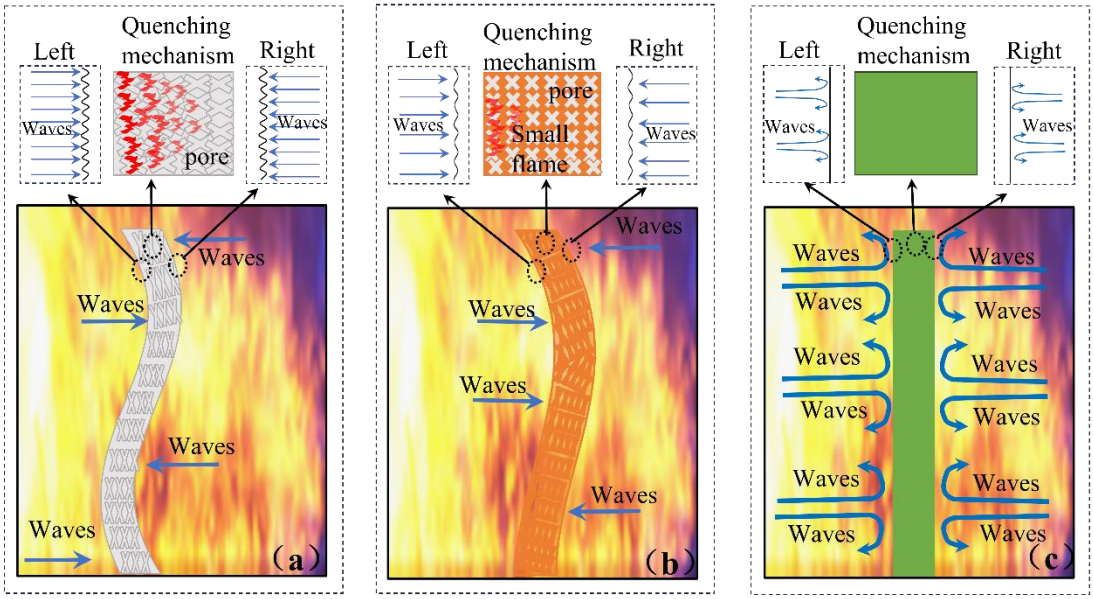

Fig. 7 Impact mechanism of structures with different elastic modulus

Conclusion

In this paper, three structures (polyurethane sponge, EPE pearl foam, carbon fiber board) are used to study the impact of different elastic modulus structure combinations on gas combustion and explosion disasters under the condition that structures with large elastic modulus must exist. The conclusions are as follows:

1. The elastic modulus of the structure has minimal impact on the structure during the early stage of flame development. The area of the flame front and the degree of deflagration also decrease with the increase of the elastic modulus. However, the disturbance degree of the airflow and flame in the pipe increases with the increase of the elastic modulus, which also increases the risk and uncertainty of gas explosion disasters.

2. The peak flame velocity at elastic modulus of 0.7 GPa and 2.8 GPa is higher than that at elastic modulus of 0.18 GPa. The energy absorption and wave suppression effect of flexible structures hinders the propagation of flames, and the peak flame velocity increases with the increase of elastic modulus. The peak flame velocity at elastic modulus of 0.7 GPa and 2.8 GPa increases by 3.56% and 7.47% compared to elastic modulus of 0.18 GPa.

3. The peak value of explosion overpressure increases with the increase of elastic modulus. Compared with the peak value of explosion overpressure under elastic modulus of 0.18 GPa, the elastic modulus of 0.7 GPa and 2.8 GPa increased by 24.63% and 42.52% in the upstream region, and 11.19% and 20.62% in the downstream region, respectively.

4. The explosion intensity and pressure rise rate increase with the increase of elastic modulus. The gas explosion intensity index under elastic modulus of 2.8 GPa is about 1.45 times that under elastic modulus of 0.18 GPa. The small elastic modulus of the structure can suppress the Helmholtz oscillation characteristics of pressure, effectively reducing the reciprocating impact of shock waves and overpressure.

In summary, in situations where structures with higher elastic modulus must exist, it is

advisable to choose structures with lower elastic modulus to form explosion-proof facilities together to ensure the safety of industrial sites.

Acknowledgements

This work was supported by the Open Foundation of the Chongqing Key Laboratory for Oil and Gas Production Safety and Risk Control (cqsrc202111); The Science and Technology Research Program of Chongqing Municipal Education Commission (Grant No. KJQN202101503); The State Key Laboratory Cultivation Base for Gas Geology and Gas Control (Henan Polytechnic University) (WS2021A04); The Science and Technology Innovation Project for Graduate Students of Chongqing Institute of Science and Technology (YKJCX2220722).

Declaration

The authors declared that there is no conflict of interest.

References

[1] Jiang H., Chi M., Hou D., Ding H., Xie Z., Zeng X., Numerical investigation and analysis of indoor gas explosion: A case study of “6·13” major gas explosion accident in Hubei Province, China, Journal of Loss Prevention in the Process Industries, 83 (2023) pp 105045.

[2] Yuanpan Z., Changgen F., Guoxun J., Xinming Q., Xinjuan L., Zhen-Yi L., Ping H., A statistical analysis of coal mine accidents caused by coal dust explosions in China, Journal of Loss Prevention in the Process Industries, 22 (2009) 4 pp 528-532.

[3] Wenhe W., Yi Q., Yue W., Zui W., Jianwe C., Underground Mine Gas Explosion Accidents and Prevention Techniques – An overview, Archives of Mining Sciences, 66 (2023) 2 pp 297–312.

[4] Zhehan W., Pierreguy A.N., Linshuang Z., A Brief Report on the Explosion on 13 June 2021 at a Market in Shiyan, China, Safety, 7 (2021) 4 pp 81-89.

[5] Wen X., Wang M., Su T., Zhang S., Pan R., Ji W., Suppression effects of ultrafine water mist on hydrogen/methane mixture explosion in an obstructed chamber, International Journal of Hydrogen Energy, 44 (2019) 60 pp 32332-32342.

[6] Duan Y., Wang S., Yang Y., Li Y., Zheng K., Experimental study on methane explosion characteristics with different types of porous media, Journal of Loss Prevention in the Process Industries, 69 (2021) pp 104370.

[7] Cao J., Wu J., Zhao Y., Cai J., Bai Y., Pang L., Suppression effects of energy-absorbing materials on natural gas explosion in utility tunnels, Energy, 281 (2023) pp 128262.

[8] Long F., Duan Y., Bu Y., Jia H., Yu S., Huang J., Promoting of foam copper with chaotic distributed pores on the deflagration of premixed hydrogen-air flame in the tube, Thermal Science, 26 (2022) 6 part B pp 5199-5209.

[9] Huang C., Chen X., Liu L., Zhang H., Yuan B., Li Y., The influence of opening shape of obstacles on explosion characteristics of premixed methane-air with concentration gradients, Process Safety and Environmental Protection, 150 (2021) pp 305-313.

[10] Yuan B., He Y., Chen X., Ding Q., Tang Y., Zhang Y., Li Y., Zhao Q., Huang C., Fang Q., Wang L., Jin H., Flame and shock wave evolution characteristics of methane explosion in a closed

horizontal pipeline filled with a three-dimensional mesh porous material, Energy, 260 (2022) pp 125137.

[11] He Y., Fang Q., Yuan B., Cao C., Zhan Y., Chen X., Huang C., Zhang Y., Ding Q., Explosion evolution behavior of methane/air premixed gas in a closed pipe filled with a bio-based porous material, Fuel, 318 (2022) pp 123716.

[12] Yu S., Duan Y., Long F., Jia H., Huang J., Bu Y., Zheng L., Fan X., The influence of flexible/rigid obstacle on flame propagation and blast injuries risk in gas explosion, Energy Sources, Part A: Recovery, Utilization, and Environmental Effects, 45 (2023) 2 pp 4520-4536.

[13] Duan Y., Yang Y., Li Y., Zhu X., Jia H., Pei B., Experimental study of premixed methane/air gas suppression by sliding porous media with different elasticity coefficients, International Communications in Heat and Mass Transfer, 126 (2021) pp 105420.

[14] R.C. Aldredge, Vaezi. V., Turbulence generation upstream of an annular premixed flame, International Communications in Heat and Mass Transfer, 26 (1999) 7 pp 919-924.

[15] Yu M., Yang X., Zheng K., Zheng L., Wen X., Experimental study of premixed syngas/air flame deflagration in a closed duct, International Journal of Hydrogen Energy, 43 (2018) 29 pp 13676-13686.

[16] Ibrahim S.S., Masri A.R., The effects of obstructions on overpressure resulting from premixed flame deflagration, Journal of Loss Prevention in the Process Industries, 14 (2001) 3 pp 213-221.

[17] Porowski R., Kowalik R., Grzmiączka M., Jurišević N., Gawdzik J., Influence of initial temperature on laminar burning velocity in hydrogen-air mixtures as potential for green energy carrier, International Communications in Heat and Mass Transfer, 146 (2023) pp 106861.

[18] Brunoro Ahumada C., Wang Q., Petersen E.L., Effects of unequal blockage ratio and obstacle spacing on wave speed and overpressure during flame propagation in stoichiometric H2/O2, Shock Waves, 30 (2020) 7-8 pp 755-767.

[19] Lv X., Zheng L., Zhang Y., Yu M., Su Y., Combined effects of obstacle position and equivalence ratio on overpressure of premixed hydrogen–air explosion, International Journal of Hydrogen Energy, 41 (2016) 39 pp 17740-17749.

[20] Petrovic J., Stamenkovic Z., Kocic M., Nikodijevic M., Porous medium magnetohydrodynamic flow and heat transfer of two immiscible fluids, Thermal Science, 20 (2016) suppl. 5 pp 1405-1417.

[21] Ou Yihong, Du Yang, Jiang Xingsheng, al. e., Study on the Thermal Ignition of Gasoline-air Mixture in Underground Oil Depots based on Experiment and Numerical Simulation, Journal of Thermal Science, 19 (2010) 2 pp 173-181.

Submitted: 05.08.2023.
Revised: 07.10.2023.
Accepted: 07.10.2023.